Letter

Breaking of Lorentz invariance caused by the interplay between spin-orbit interaction and transverse phonon modes in quantum wires

D. V. Efremov,[1] Weyner Ccuiro,[2,3] Luis E. F. Foa Torres,[4] and M. N. Kiselev[3]
[1]IFW Dresden, Helmholtzstr. 20, 01069 Dresden, Germany
[2]International School for Advanced Studies (SISSA), via Bonomea 265, I-34136 Trieste, Italy
[3]The Abdus Salam International Centre for Theoretical Physics, Strada Costiera 11, I-34151 Trieste, Italy
[4]Departamento Fısica, Facultad de Ciencias Fısicas y Matematicas, Universidad de Chile, Santiago 837.0415, Chile

(Received 23 July 2024; accepted 25 March 2025; published 14 April 2025)

We investigate Lorentz invariance breaking in quantum wires due to Rashba spin-orbit interaction and transverse phonons. Using bosonization, we derive an effective action coupling electronic and mechanical degrees of freedom. Strikingly, at a quantum phase transition between straight and bent wire states, we find a gapped phonon mode and a gapless mode with quadratic dispersion, signaling the breaking of Lorentz invariance. We explore stability conditions for general potentials and propose nanomechanical back action as a sensitive tool for detecting this transition, with implications for sliding Luttinger liquids and dimensional crossover studies.

DOI: 10.1103/PhysRevResearch.7.L022016

Introduction and overview of key findings. Physics shows a surprising hierarchy of alternating Lorentz and Galilean invariance, a fundamental principle governing the behavior of objects moving at relativistic speeds. As we descend to nonrelativistic energies, the Lorentz invariance gives way to Galilean invariance. Intriguingly, in condensed matter physics, lower energy excitations once again obey Lorentz invariance. A prime example is the quasiparticles in one-dimensional systems [1,2]. Here, electrons are described by the Luttinger liquid model [3–5] whose excitations are bosons, obeying Lorentz invariance. Similarly, the mechanical degrees of freedom, described by phonons, also demonstrate Lorentz invariance.

Nanoelectromechanical systems have captivated researchers for decades [6], offering a wide array of potential applications and research avenues. Their small size and high sensitivity make them invaluable tools in novel microelectronics [7–9]. At the cutting edge are ultrathin membranes and nanowires, fabricated from diverse materials including silicon [10,11], metals [12], graphene [13], carbon nanotubes [14], and many others [8]. These systems now operate in the quantum-mechanical regime, where the behavior of the electronic component, when considered in isolation, is well understood. The most pronounced quantum-mechanical effects manifest in lower-dimensional systems, particularly nanowires. It is well established that many one-dimensional systems are accurately described by the Luttinger liquid model [1,2,15,16]. Theoretical [17–20] and experimental studies [21,22] also point out Luttinger liquid physics in dimensions larger than one, with recent experiments in twisted bilayer tungsten ditelluride ($tWTe_2$) [23] which inspired further theory efforts [24]. However, to further advance these devices, it is crucial to comprehend the quantum effects arising from the coupling between mechanical motion and electric current. Recent interest has also focused on the interactions between electrons and bosonic modes in cavities [25–27], expanding our understanding of these systems.

The coupling of the electrons of the nanowire in an external magnetic field with the elastic modes of the wire was first considered by Ahn and co-authors [28–30]. In this model, the coupling of the electric charge Luttinger liquid with the elastic modes of the nanowire occurs due to the Lorentz force as a result of the perpendicular displacements of the wire in the magnetic field.

In this Letter we propose a different setup in which a synthetic magnetic field associated with the Rashba spin-orbit interaction is used as a tool to control quantum transport through a quantum wire. The construction of our setup (see Fig. 1) is similar to those used in recent experiments, e.g., to one based on an InAs suspended nanowire that was recently studied in [22]. For our setup, we study how the spin current in the presence of the Rashba spin-orbit interaction couples to elastic modes of the wire that arise due to transverse displacements. We show that as a result of the interaction, the two corresponding Goldstone modes corresponding to the Luttinger liquid and the elastic modes, transform into a Higgs boson and a Goldstone mode with quadratic dispersion. This leads to intriguing physical phenomena, including the breaking of Lorentz invariance under specific conditions. We derive an effective action using bosonization techniques, and explore the resulting mode structure and stability conditions under various potential parameters.

Hamiltonian model. The key component of the model considered here is the Rashba spin-orbit interaction arising from the external potential. It is described by the following

Published by the American Physical Society under the terms of the Creative Commons Attribution 4.0 International license. Further distribution of this work must maintain attribution to the author(s) and the published article's title, journal citation, and DOI.

Hamiltonian for a single electron:

$$\hat{H} = \frac{\hat{p}^2}{2m} + \alpha_{so}(\hat{\vec{p}} \times \vec{\sigma}) \cdot \nabla U(y,z) + U(y,z), \tag{1}$$

where $\hat{\vec{p}}$ is the momentum operator, m stands for the electron mass, α_{so} denotes the Rashba spin-orbit coupling strength, $\vec{\sigma}$ represents the Pauli matrices which describe the electron's spin, and $U(y,z)$ is the spatially dependent confining potential. It's important to note that the electric field $\vec{E} = -\nabla U(y,z)$, representing the gradient of the potential, is nonvanishing due to the absence of inversion symmetry in the system.

Following [31] we assume the external potential as

$$U(y,z) = b_y y^2/2 + b_z z^2/2 + cyz. \tag{2}$$

By a special choice of the potential $U(y,z)$ it is possible to bring the single-particle Hamiltonian Eq. (1) into a quadratic form, similar to the model of N electrons moving in a synthetic magnetic field and described by the Hamiltonian $h = 1/(2m)(\hat{p}_x - A_x)^2$. One should note, however, that this synthetic magnetic field is not breaking time-reversal symmetry and therefore preserves Kramers' degeneracy. In our problem, it is realized with the following conditions:

$$2b_{y,z} = \left(m\alpha_{so}^2\right)^{-1} \pm \sqrt{\left(m\alpha_{so}^2\right)^{-2} - 4c^2}, \tag{3}$$

where c is kept as a free parameter. Under this condition the Hamiltonian takes the following form:

$$\hat{H} = \frac{1}{2m}(\hat{p}_x + m\alpha_{so}[(b_z z + cy)\sigma_y - (b_y y + cz)\sigma_z])^2. \tag{4}$$

Here and below we assume that the local x axis is along the wire and that the deviation from the equilibrium position is small, keeping only the quadratic terms of the deviation from equilibrium.

To demonstrate the basic properties of the dynamical model with a synthetic magnetic field, we choose $b_y = b_z = c = (2m\alpha_{so}^2)^{-1}$. Rotation in the spin $(\sigma_y - \sigma_z)\sqrt{2} \to \sigma_z$, $(\sigma_y + \sigma_z)\sqrt{2} \to \sigma_y$ and the coordinate space $(z+y)/\sqrt{2} \to y$, $(y - z)/\sqrt{2} \to z$ simplify the equation to the form

$$\hat{H} = \frac{1}{2m}\left(\hat{p}_x + \frac{1}{\alpha_{so}}\sigma_z y\right)^2. \tag{5}$$

With this, the electronic part of the Hamiltonian can be written as

$$H_e = \frac{1}{2m}\sum_{\alpha,\beta=\pm}\int dx \Psi_\alpha^\dagger(x)\left(\hat{p}_x + \frac{1}{\alpha_{so}}u_y\sigma_\alpha^z\right)^2\Psi_\alpha(x) + \frac{1}{2}\int dx dx' V(x-x')\rho(x)\rho(x'),$$

where $u_y(x) = y(x) - y_0$ is a y component of the transverse displacements from the equilibrium position y_0 (see Fig. 1). The second term describes the density-density interaction. Here $\rho(x) = \sum_{\alpha=\pm}\Psi_\alpha^\dagger(x)\Psi_\alpha(x)$ and $V(x-x')$ is the electron-electron interaction. There are also other possible consequences of spin-orbit interaction such as those considered in [32]. They are beyond our present scope.

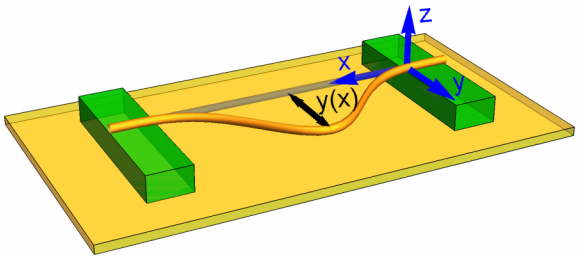


FIG. 1. Schematic representation of the experimental setup. The orange beam represents a suspended double clamped nanowire with a displacement $y(x)$. Green supports can also be used as electric contacts.

After the standard procedure of bosonization, the Hamiltonian [1,2] takes the following form:

$$H_e = \sum_{s=\pm}\frac{v}{2\pi}\int dx\left(g\left(\partial_x\theta_s - \alpha_{so}^{-1}\sigma_z u_y\right)^2 + g^{-1}(\partial_x\phi_s)^2\right),$$

where $v = v_F/g$ is the electronic velocity and v_F is Fermi velocity. For short-range interaction $V(x-x') = V\delta(x-x')$, g is given by $g = (1 + V/(\pi v_F))^{-1/2}$. For simplicity we assume $g = 1$. The full expression can be easily recovered.

The mechanical degrees of freedom is given by the elastic response of the wire on the transversal strain. We study a one-dimensional suspended double clamped beam of mass density ρ_m and stiffness $\mathbb{T}$ extending along the x direction. We assume that $y_0(x) = z_0(x) = 0$ corresponds to equilibrium. The mechanical part is related to the strain in the beam, which is associated with small transverse displacements along the y and z axes from the equilibrium position: $u_y(x) = y(x) - y_0$ and $u_z(x) = z(x) - z_0$. The corresponding energy depends on the gradient of the displacements, and its behavior is captured by the Hamiltonian

$$H_u = \sum_{\zeta=y,z}\int dx\left(\frac{\pi_\zeta^2}{2\rho_m} + \frac{\mathbb{T}}{2}\left(\frac{\partial u_\zeta}{\partial x}\right)^2\right). \tag{6}$$

Here $\pi_\zeta(x)$ are the conjugated momenta of $u_\zeta(x)$, $\zeta = y,z$, satisfying the commutation relations $[u_\zeta(x), \pi_{\zeta'}(x')] = i\delta(x-x')\delta_{\zeta\zeta'}$.

Effective action. Using the canonical transformation we get the action from the Hamiltonian. It takes the form

$$S = S_{LL} + S_u + S_{LL-u},$$

$$S_{LL} = \frac{v}{2\pi g}\sum_{\alpha=\pm}\int_0^\beta d\tau\int_{-\infty}^{\infty} dx(v^{-2}(\partial_\tau\phi_\alpha)^2 + (\partial_x\phi_\alpha)^2),$$

$$S_u = \frac{\mathbb{T}}{2}\sum_{\eta=y,z}\int_0^\beta d\tau\int_{-\infty}^{\infty} dx\left(v_s^{-2}(\partial_\tau u_\eta)^2 + (\partial_x u_\eta)^2\right),$$

$$S_{LL-u} = -\frac{i\alpha_{so}}{\pi}^{-1}\int_0^\beta d\tau\int_{-\infty}^{\infty} dx(\partial_\tau\phi_+ - \partial_\tau\phi_-)u_y. \tag{7}$$

$v_s = \sqrt{\mathbb{T}/\rho_m}$ is the phonon sound velocity and $\beta = 1/T$. Here we would like to note that the last term corresponds to the coupling of the transverse displacement to the spinor current $J = \frac{e}{mc\alpha_{so}}(\partial_t\phi_+ - \partial_t\phi_-)$, which emerges due to deviation of the beam from the equilibrium. It is worth to introduce new

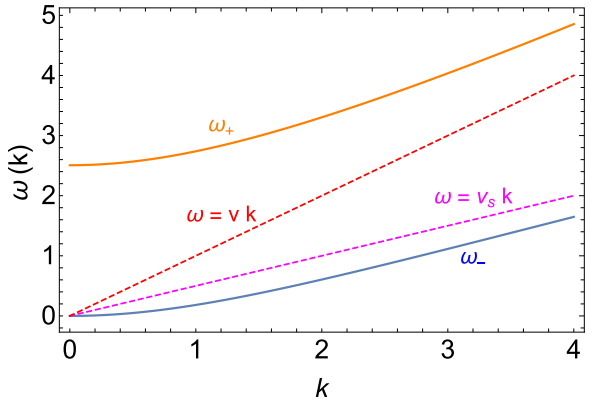


FIG. 2. Eigenmodes $\omega_{\pm}(k)$ (solid lines). The dashed lines denote the bosonic mode for electron $\omega = vk$, phonon $\omega = v_s k$.

fields $\phi_c + \phi_s$:

$$\phi_c = \frac{1}{\sqrt{2}}(\phi_+ + \phi_-), \qquad \phi_s = \frac{1}{\sqrt{2}}(\phi_+ - \phi_-),$$

which describe the charge and spin degrees of freedom, respectively.

The Euclidean action can be written as

$$S = \sum_k \sum_{\omega_n} \sum_{\alpha=c,s} \frac{v}{2\pi g}\left(\frac{\omega_n^2}{v^2} + k^2\right)\phi^*_{nk,\alpha}\phi_{nk,\alpha} + \sum_k \sum_{\omega_n} \sum_{\zeta=y,z} \frac{\mathbb{T}}{2}\left(\frac{\omega_n^2}{v_s^2} + k^2\right)u^*_{nk,\zeta}u_{nk,\zeta} + \sum_k \sum_{\omega_n} \sum_{\zeta=y,z} \frac{\sqrt{2}\alpha_{so}^{-1}\omega_n}{2\pi}(u_{nk,y}\phi^*_{nk,s} - u^*_{nk,y}\phi_{nk,s}). \quad (8)$$

From four modes of this action, two are decoupled: the transverse phonon mode along the z-direction with dispersion $\omega = v_s k$ and the charge mode of the Luttinger liquid with dispersion $\omega = vk$. The other two, the spin mode of the Luttinger liquid and the transverse phonon mode along the y direction, give a gapped transverse phonon mode with dispersion $\omega_+^2 = \frac{1}{2}((v_s^2 + v^2)k^2 + \Delta^2) + \sqrt{((v_s^2 + v^2)k^2 + \Delta^2)^2 - 4v_s^2v^2k^4}$, where $\Delta^2 = 2v_F/(\pi\rho_m\alpha_{so}^2)$, and a gapless mode $\omega_-^2 = \frac{1}{2}((v_s^2 + v^2)k^2 + \Delta^2) - \sqrt{((v_s^2 + v^2)k^2 + \Delta^2)^2 - 4v_s^2v^2k^4}$ (see Fig. 2). The gapless mode reflects the breaking of the Lorentz invariance of the bosonic mode of the Luttinger liquid. Instead of the linear dispersion, which corresponds to the Lorentz invariance of the Luttinger liquid, the dispersion is $\omega_- \sim k^2$, which corresponds to the Galilean invariance.

General case. Now we explore the effect of the case without the constraint, Eq. (3). Then

$$\hat{H} = \frac{1}{2m}(\hat{p}_x + m\alpha_{so}[(b_z z + cy)\sigma_y - (b_y y + cz)\sigma_z])^2 + \tilde{U}(y,z)$$

with

$$\tilde{U}(y,z) = U(y,z) - \frac{m\alpha_{so}^2}{2}[(b_y y + cz)^2 + (b_z z + cy)^2]. \quad (9)$$

Negative $\tilde{U}(y,z)$ leads to a shift of the position of the equilibrium of the beam, $u_{y,z}(0) \neq 0$. A simple calculation leads to the following conditions for stability of the system:

$$b_y - m\alpha_{so}^2(b_y^2 + c^2) > 0, \quad b_z - m\alpha_{so}^2(b_z^2 + c^2) > 0$$
$$(c(1 - m\alpha_{so}^2(b_y + b_z)))^2 < (b_z - m\alpha_{so}^2(b_z^2 + c^2)) \times (b_y - m\alpha_{so}^2(b_y^2 + c^2)). \quad (10)$$

We introduce small transverse displacements as $z - z_0 = r\cos\varphi$ and $y - y_0 = r\sin\varphi$. For rotation in spin space we get

$$\hat{H} = \frac{1}{2m}(\hat{p}_x + \Lambda r\sigma_z)^2 + \tilde{U} \quad (11)$$

with

$$\frac{\Lambda}{(m\alpha_{so})} = [(b_y\sin\varphi + c\cos\varphi)^2 + (b_z\cos\varphi + c\sin\varphi)^2]^{1/2}.$$

The effective potential is

$$\tilde{U} = r^2\frac{K(\varphi)}{2} \quad (12)$$

with

$$K(\varphi) = \frac{\tilde{b}_z + \tilde{b}_y}{2} + \left[\left(\frac{\tilde{b}_z - \tilde{b}_y}{2}\right)^2 + \tilde{c}^2\right]^{1/2}\cos(2\varphi - \varphi_0) - c^2 m\alpha_{so}^2, \quad (13)$$

where $\tan\varphi_0 = \frac{2\tilde{c}}{\tilde{b}_z - \tilde{b}_y}$ and

$$\tilde{b}_z = b_z(1 - m\alpha_{so}^2 b_z), \qquad \tilde{b}_y = b_y(1 - m\alpha_{so}^2 b_y)$$
$$\tilde{c}_z = c(1 - m\alpha_{so}^2(b_z + b_y)). \quad (14)$$

We choose the new axes along the direction $2\varphi = \varphi_0$ and $2\varphi = \varphi_0 + \pi$, and y' and z'. The minimum of the effective potential corresponds to the direction of the z' -axis. The effective external potential Eq. (12) depends on the transverse displacements. It leads to the renormalization of the action of the mechanical degrees of the beam if $K(\varphi_0/2 + \pi/2) = 0$ is the quantum critical point (see Fig. 3). The condition Eq. (3) corresponds to $K(\varphi_0/2 + \pi/2) < 0$. For $K(\varphi_0/2 + \pi/2) > 0$ the vacuum is trivial, while for $K(\varphi_0/2 + \pi/2) < 0$ one needs to rederive the effective action with nontrivial vacuum $u_{y_0} \neq 0$.

Negative $K(\varphi)$ can be attributed to a nontrivial vacuum of the system while the vacuum for positive $K(\varphi)$ is trivial. In both cases, away from the quantum critical point, Lorentz invariance is preserved and the spectrum of the lowest energy Goldstone mode $\omega \propto k$. The Lorentz invariance is broken at the quantum critical point resulting Galilean invariant Goldstone mode being $\omega \propto k^2$.

Using the standard procedure we come to the action

$$S = \sum_k \sum_{\omega_n} \sum_{\alpha=c,s} \frac{v}{2\pi g}\left(\frac{\omega_n^2}{v^2} + k^2\right)\phi^*_{nk,\alpha}\phi_{nk,\alpha} + \sum_k \sum_{\omega_n} \sum_{\zeta=y',z'} \frac{\mathbb{T}}{2}\left(\frac{\omega_n^2}{v_s^2} + k^2 + \frac{K(\varphi_\zeta)}{\mathbb{T}}\right)u^*_{nk,\zeta}u_{nk,\zeta} + \sum_k \sum_{\omega_n} \sum_{\zeta=y',z'} \frac{\Lambda\omega_n}{2\pi}(u_{nk,\zeta}\phi^*_{nk,s} - \text{H.c.}). \quad (15)$$

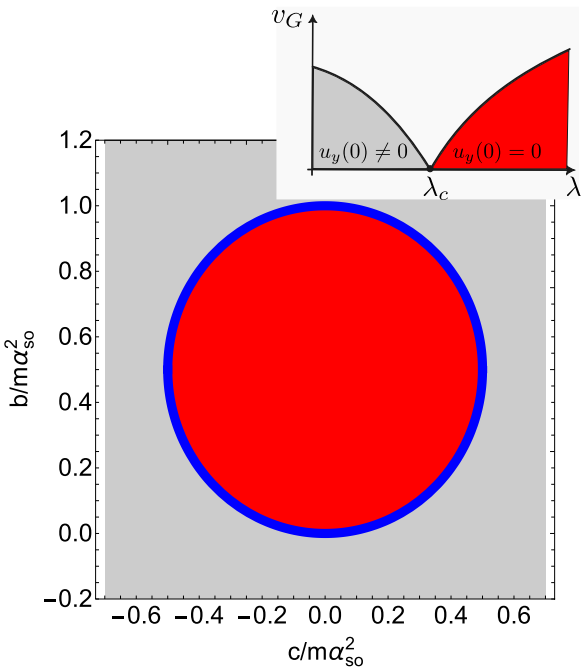


FIG. 3. Schematic phase diagram of possible coefficients $b = b_{z,y}$ vs c. The critical region is in blue. The outside gray area corresponds to the region of instability. The inset represents the same transition as a function of $\lambda = K(\phi_0/2 + \pi/2)$. Here v_G is a sound velocity of the Goldstone mode ω_- which vanishes at the quantum critical point.

Correlation functions. To see the consequences of the coupling between the electronic and mechanical degrees of freedom, we calculate the correlation functions $\langle u_z(q, \omega_n) u_z(q, \omega_n)\rangle$ and $\langle \phi_c(q, \omega_n)\phi_c(q, \omega_n)\rangle$. To focus on the most important features of the coupling, assuming that the stiffness of the mechanical degrees of freedom is strongly anisotropic, leads to the survival of only one of the mechanical modes. This assumption results in a linear polarization of the mechanical motion. The general case will be considered elsewhere.

Using the standard procedure of integration of complimentary degrees of freedom, we get

$$\left\langle u^*_{k\omega_n\xi} u_{k\omega_n\xi}\right\rangle = \frac{1}{\rho_m}\frac{\left(\omega_n^2 + v^2k^2\right)}{D} \tag{16}$$

and

$$\left\langle \phi^*_{k\omega_n,s}\phi_{k,\omega_n,s}\right\rangle = \frac{\pi v_F\left(\omega_n^2 + v_s^2k^2 + K/\rho_m\right)}{D}, \tag{17}$$

where

$$D = \left(\left(\omega_n^2 + v^2k^2\right)\left(\omega_n^2 + v_s^2k^2 + K/\rho_m\right) + \tilde{\omega}^2\omega_n^2\right) \tag{18}$$

and $\tilde{\omega}^2 = \Lambda^2 v_F/(\pi\rho_m)$.

Performing analytical continuation we get the correspondent response functions. The imaginary parts of the response functions are shown in Fig. 4.

Mechanical back action as a tool for quantum spectroscopy of the Luttinger liquids. One sees by comparing plots of mechanical correlation functions on Fig. 4 at (a), (b) and away (e), (f) from the QCP that the character of the Goldstone mode spectrum (quadratic vs linear) and the redistribution of the low frequency spectral weight allows to identify the position of the QPT (see the inset of Fig. 3) with a high accuracy even without measuring the quantum transport correlation functions (c), (g)

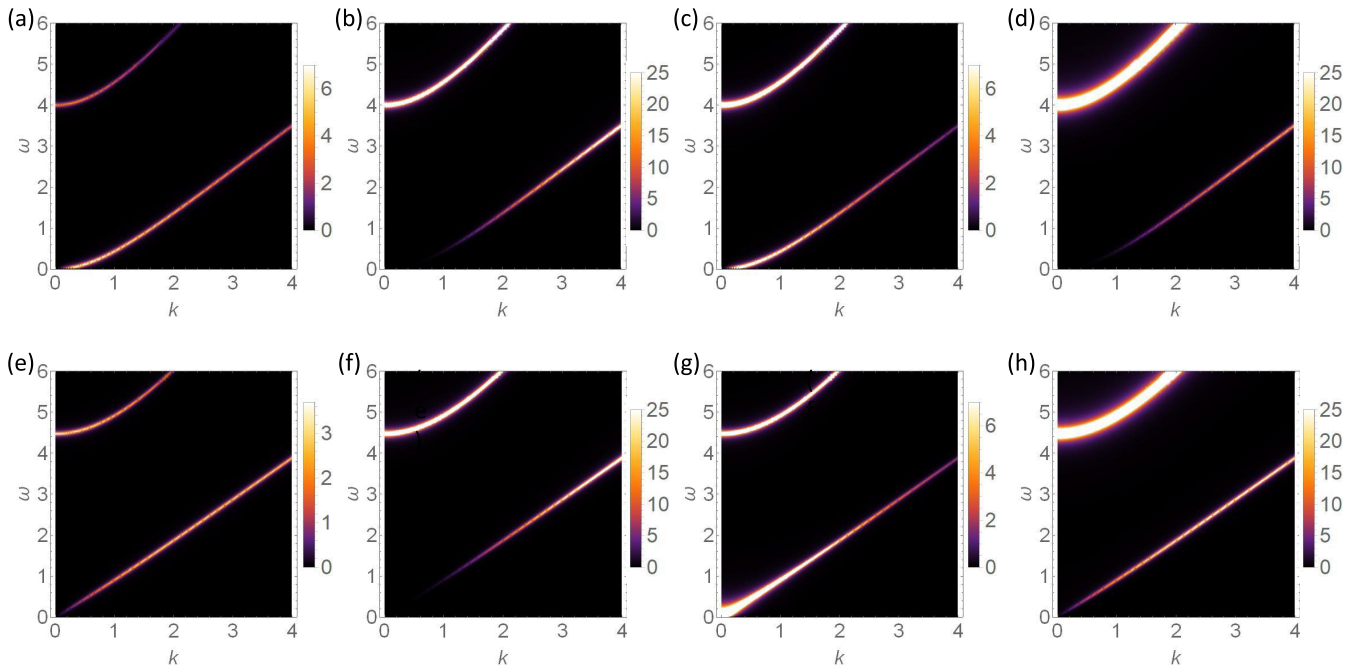


FIG. 4. Correlations functions (a) $Im\langle u^*_y(k, \omega)u_y(k, \omega)\rangle$; (b) $\omega^2 Im\langle u^*_y(k, \omega)u_y(k, \omega)\rangle$; (c) $Im\langle\phi^*_s(k, \omega)\phi_s(k, \omega)\rangle$; and (d) $\omega^2 Im\langle\phi^*_s(k, \omega)\phi_s(k, \omega)\rangle$ at the position of the quantum critical point. Plots (e)–(h) show the same correlations functions as in (a)–(c) away from the quantum critical point (see the phase diagram on Fig. 3). The parameters are $v_s = 1$, $v_F = 2$, $\rho = 1$, $\Lambda = 1$. Parameter $K = 0$ for (a)–(d) and $K = 4$ for (e)–(h).

and (d), (h) which provide complementary information about corresponding Goldstone spectra and the spectral weights. The mechanical back action information is important, as the Rashba spin-orbit interaction can be responsible for opening a gap in the charge bosonic correlation function which in turn will influence the elastic Goldstone modes. Yet another interesting question is related to behavior of either driven or excited mechanical systems being associated with effects of controllable nonlinearity of elastic modes (interaction effects), possibility of parametric amplification, and dissipative dynamics associated with mechanical quality factor (friction). Experimental realization of setup Fig. 1 is discussed in [33].

Final remarks and conclusions. Similar breaking of Lorentz invariance at quantum critical points appears in two-species Bose gas mixtures with density-density repulsive interactions [34]. With $U(1) \times U(1)$ symmetry broken independently in noninteracting species, intercomponent coupling lifts the twofold degeneracy of soundlike modes [34], leading to vanishing sound velocity and quadratic dispersion $\omega \sim k^2$ (see also discussion about type I and type II Goldstone modes in [35,36]). The nontrivial vacuum shows phase separation [34,37] via Bogoliubov-de Gennes equations [34]. Other examples include 1D Bose-Hubbard systems [38–40] and two-component Luttinger liquids [41,42], where emergent S U (2) symmetry at QCP breaks Lorentz invariance, describable by nonlinear sigma models [43].

From a single wire to few coupled quantum wires. The single-wire model presented here advances understanding of quantum wire arrays coupled by tunneling or interaction in mechanically driven sliding Luttinger liquids (SLL). Progress toward SLLs and dimensional crossover requires understanding quantum noise in coupled wires, analogous to co-propagating edge modes in IQH $\nu = 2$ devices [44]. Nanomechanically coupled SLLs enable study of electronic-elastic coupling in topological insulators, with transitions achievable through tunneling [15,31] or interactions [31].

In summary, we analyzed a nanomechanical system coupling transverse elastic modes to electronic degrees via Rashba spin-orbit interaction. We found a quantum phase transition between straight and bent wire states, characterized by Lorentz invariance breaking and quadratic Goldstone mode dispersion. Our findings suggest that measuring the back action of the nanomechanical system provides a highly sensitive and efficient spectroscopic tool for detecting the QPT position, complementing quantum transport experiments. We hope that our proposal may trigger new experiments with suspended nanowires.

Acknowledgments. We thank B. L. Altshuler, Ya. Blanter, A. Chubukov, Y. Gefen, Th. Giamarchi, D. Maslov, C. Mora, F. von Oppen, S. Sachdev, and J. Schmalian for fruitful discussions. The work of M.N.K. is conducted within the framework of the Trieste Institute for Theoretical Quantum Technologies (TQT) and supported in part by the NSF under Grants No. NSF PHY-1748958 and No. PHY-2309135. M.N.K. acknowledges support of the IHP (UAR 839 CNRS-Sorbonne Universite) and LabEx CARMIN (ANR-10LABX-59-01) L.E.F.F.T. acknowledges financial support by ANID FONDECYT (Chile) through Grant No. 1211038, The Abdus Salam International Center for Theoretical Physics and the Simons Foundation, and by the EU Horizon 2020 research and innovation program under the Marie-Sklodowska-Curie Grant Agreement No. 873028 (HYDROTRONICS Project). D.V.E. acknowledges the financial support of DFG (Grants No. 529677299 and No. 449494427) and hospitality of Abdus Salam International Center for Theoretical Physics.

[1] A. O. Gogolin, A. A. Nersesyan, and A. M. Tsvelik, *Bosonization and Strongly Correlated Systems* (Cambridge University Press, Cambridge, 2004).

[2] T. Giamarchi, *Quantum Physics in One Dimension*, International series of monographs on physics (Clarendon Press, Oxford, 2004).

[3] J. M. Luttinger, An exactly soluble model of a many-fermion system, J. Math. Phys. **4**, 1154 (1963).

[4] D. C. Mattis and E. H. Lieb, Exact solution of a many-fermion system and its associated Boson field, J. Math. Phys. **6**, 304 (1965).

[5] F. D. M. Haldane, Effective harmonic-fluid approach to low-energy properties of one-dimensional quantum fluids, Phys. Rev. Lett. **47**, 1840 (1981).

[6] A. N. Cleland, *Foundations of Nanomechanics* (Springer Berlin, Heidelberg, New York, 2003).

[7] J. Zhu, X. Liu, Q. Shi, T. He, Z. Sun, X. Guo, W. Liu, O. B. Sulaiman, B. Dong, and C. Lee, Development trends and perspectives of future sensors and MEMS/NEMS, Micromachines **11** (2020).

[8] C.-Y. Hsu, A. M. Rheima, Z. sabri Abbas, M. U. Faryad, M. M. Kadhim, U. S. Altimari, A. H. Dawood, A. dhari jawad albayati, Z. T. Abed, R. S. Radhi, A. S. Jaber, S. K. Hachim, F. K. Ali, Z. H. Mahmoud, G. Behzadi pour, and E. Kianfar, Nanowires properties and applications: A review study, S. Afr. J. Chem. Eng. **46**, 286 (2023).

[9] A. Haroun, X. Le, S. Gao, B. Dong, T. He, Z. Zhang, F. Wen, S. Xu, and C. Lee, Progress in micro/nano sensors and nanoenergy for future AIoT-based smart home applications, Nano Express **2**, 022005 (2021).

[10] M. M. Roberts, L. J. Klein, D. E. Savage, K. A. Slinker, M. Friesen, G. Celler, M. A. Eriksson, and M. G. Lagally, Elastically relaxed free-standing strained-silicon nanomembranes, Nat. Mater. **5**, 388 (2006).

[11] C. C. Striemer, T. R. Gaborski, J. L. McGrath, and P. M. Fauchet, Charge- and size-based separation of macromolecules using ultrathin silicon membranes, Nature (London) **445**, 749 (2007).

[12] J. Jin, Y. Wakayama, X. Peng, and I. Ichinose, Surfactant-assisted fabrication of free-standing inorganic sheets covering an array of micrometre-sized holes, Nat. Mater. **6**, 686 (2007).

[13] C. Lee, X. Wei, J. W. Kysar, and J. Hone, Measurement of the elastic properties and intrinsic strength of monolayer graphene, Science **321**, 385 (2008).

[14] S. Raychaudhuri and E. T. Yu, Critical dimensions in coherently strained coaxial nanowire heterostructures, J. Appl. Phys. **99**, 114308 (2006).

[15] C. L. Kane and M. P. A. Fisher, Transport in a one-channel luttinger liquid, Phys. Rev. Lett. **68**, 1220 (1992).

[16] H. J. Schulz, G. Cuniberti, and P. Pieri, Fermi Liquids and Luttinger Liquids, in *Field Theories for Low-Dimensional Condensed Matter Systems* (Springer, Berlin, Heidelberg, 2000).

[17] P. W. Anderson, Hall effect in the two-dimensional Luttinger liquid, Phys. Rev. Lett. **67**, 2092 (1991).

[18] X. G. Wen, Metallic non-Fermi-liquid fixed point in two and higher dimensions, Phys. Rev. B **42**, 6623 (1990).

[19] V. J. Emery, E. Fradkin, S. A. Kivelson, and T. C. Lubensky, Quantum theory of the smectic metal state in stripe phases, Phys. Rev. Lett. **85**, 2160 (2000).

[20] S. L. Sondhi and K. Yang, Sliding phases via magnetic fields, Phys. Rev. B **63**, 054430 (2001).

[21] G. Badawy, S. Gazibegovic, F. Borsoi, S. Heedt, C.-A. Wang, S. Koelling, M. A. Verheijen, L. P. Kouwenhoven, and E. P. A. M. Bakkers, High mobility stemless InSb nanowires, Nano Lett. **19**, 3575 (2019).

[22] A. Iorio, M. Rocci, L. Bours, M. Carrega, V. Zannier, L. Sorba, S. Roddaro, F. Giazotto, and E. Strambini, Vectorial control of the spin-orbit interaction in suspended InAs nanowires, Nano Lett. **19**, 652 (2019).

[23] Y.-M. Wu, C. Murthy, and S. A. Kivelson, Possible sliding regimes in twisted bilayer WTe_2, Phys. Rev. Lett. **133**, 246501 (2024).

[24] G. Yu, P. Wang, A. J. Uzan-Narovlansky, Y. Jia, M. Onyszczak, R. Singha, X. Gui, T. Song, Y. Tang, K. Watanabe, T. Taniguchi, R. J. Cava, L. M. Schoop, and S. Wu, Evidence for two dimensional anisotropic Luttinger liquids at millikelvin temperatures, Nat. Commun. **14**, 7025 (2023).

[25] D.-P. Nguyen, G. Arwas, Z. Lin, W. Yao, and C. Ciuti, Electron-photon Chern number in cavity-embedded 2D Moiré materials, Phys. Rev. Lett. **131**, 176602 (2023).

[26] G. Arwas and C. Ciuti, Quantum electron transport controlled by cavity vacuum fields, Phys. Rev. B **107**, 045425 (2023).

[27] D.-P. Nguyen, G. Arwas, and C. Ciuti, Electron conductance and many-body marker of a cavity-embedded topological 1D chain, Phys. Rev. B **110**, 195416 (2024).

[28] K.-H. Ahn and H. Yi, Elementary excitations in one-dimensional electromechanical systems; transport with back-reaction, Europhys. Lett. **67**, 641 (2004).

[29] K.-J. Kim and K.-H. Ahn, Excitation gap of a nano-electromechanical rod in magnetic fields, Physica E **40**, 1412 (2008).

[30] H. Yi and K.-H. Ahn, Dynamical electron transport through a nanoelectromechanical wire in a magnetic field, Eur. Phys. J. B **76**, 283 (2010).

[31] R. A. Santos, C.-W. Huang, Y. Gefen, and D. B. Gutman, Fractional topological insulators: From sliding Luttinger liquids to Chern-simons theory, Phys. Rev. B **91**, 205141 (2015).

[32] V. Gritsev, G. Japaridze, M. Pletyukhov, and D. Baeriswyl, Competing effects of interactions and spin-orbit coupling in a quantum wire, Phys. Rev. Lett. **94**, 137207 (2005).

[33] InSb and InAs nanowires [21,22] provide ideal platforms, with InSb showing strong Rashba spin-orbit interaction ($|g| \sim 50$), high mobility (7.7×10^4 cm^2/VS, $T = 300$ K), and $\alpha_R = 0.45 - 0.64$ eV Å. InAs offers viable alternatives with $|g| \sim 10$ and mobility $\sim 1 - 2 \times 10^4$ cm^2/VS [22].

[34] A. S. Alexandrov and V. V. Kabanov, Excitations and phase segregation in a two-component Bose-Einstein condensate with an arbitrary interaction, J. Phys.: Condens. Matter **14**, L327 (2002).

[35] H. Watanabe and H. Murayama, Unified description of Nambu-Goldstone bosons without Lorentz invariance, Phys. Rev. Lett. **108**, 251602 (2012).

[36] J.-S. Pan, W. V. Liu, and X.-J. Liu, Emergence of the unconventional type-II Nambu-Goldstone modes with topological origin in Bose superfluids, Phys. Rev. Lett. **125**, 260402 (2020).

[37] M.-C. Chung and A. B. Bhattacherjee, Dynamical structure factor and spin-density separation for a weakly interacting two-component Bose gas, Phys. Rev. Lett. **101**, 070402 (2008).

[38] M. P. A. Fisher, P. B. Weichman, G. Grinstein, and D. S. Fisher, Boson localization and the superfluid-insulator transition, Phys. Rev. B **40**, 546 (1989).

[39] M. B. Zvonarev, V. V. Cheianov, and T. Giamarchi, Spin dynamics in a one-dimensional ferromagnetic Bose gas, Phys. Rev. Lett. **99**, 240404 (2007).

[40] M. B. Zvonarev, V. V. Cheianov, and T. Giamarchi, Dynamical properties of the one-dimensional spin-1/2 Bose-Hubbard model near a Mott-insulator to ferromagnetic-liquid transition, Phys. Rev. Lett. **103**, 110401 (2009).

[41] J. S. Meyer, K. A. Matveev, and A. I. Larkin, Transition from a one-dimensional to a quasi-one-dimensional state in interacting quantum wires, Phys. Rev. Lett. **98**, 126404 (2007).

[42] M. Sitte, A. Rosch, J. S. Meyer, K. A. Matveev, and M. Garst, Emergent Lorentz symmetry with vanishing velocity in a critical two-subband quantum wire, Phys. Rev. Lett. **102**, 176404 (2009).

[43] E. Fradkin, *Field Theories of Condensed Matter Physics* (Cambridge University Press, Cambridge, 2013).

[44] Mirco Milletarì and B. Rosenow, Shot-noise signatures of charge fractionalization in the $\nu = 2$ quantum Hall edge, Phys. Rev. Lett. **111**, 136807 (2013).